

# Reversibility of $\text{Na}^+/\text{Mg}^{2+}$ antiport in rat erythrocytes

Theodor Günther<sup>\*</sup>, Jürgen Vormann

*Institute of Molecular Biology and Biochemistry, Free University of Berlin, Arnimallee 22, D-14195 Berlin, Germany*

Received 22 June 1994; accepted 11 November 1994

## Abstract

Rat erythrocytes loaded with  $\text{Mg}^{2+}$  plus  $\text{Na}^+$  performed  $\text{Mg}^{2+}$  uptake under an intracellular/extracellular  $\text{Na}^+$  gradient.  $\text{Mg}^{2+}$  uptake was coupled to  $\text{Na}^+$  release at a stoichiometric ratio of  $1 \text{ Mg}^{2+}/2 \text{ Na}^+$ .  $\text{Mg}^{2+}$  uptake was inhibited by amiloride, imipramine and quinidine.  $\text{Mn}^{2+}$  was taken up by the same transporter as  $\text{Mg}^{2+}$ . Similar results had been found for net  $\text{Mg}^{2+}$  efflux via  $\text{Na}^+/\text{Mg}^{2+}$  antiport in such rat erythrocytes. Hence, it can be concluded that  $\text{Na}^+/\text{Mg}^{2+}$  antiport in  $\text{Mg}^{2+}$ -loaded rat erythrocytes operates reversibly according to the direction of the  $\text{Na}^+$  gradient which is a contributing driving force. Net  $\text{Mg}^{2+}$  influx was dependent on ATP which increased the affinity of intracellular  $\text{Mg}^{2+}$  by activating  $\text{Na}^+/\text{Mg}^{2+}$  antiport.  $\text{Mg}^{2+}$  uptake was increased by phorbol ester and inhibited by staurosporine, indicating that ATP may function via protein phosphorylation by protein kinase C.

**Keywords:** Sodium ion; Magnesium ion; Antiport; Amiloride; Protein kinase C; (Rat erythrocyte)

## 1. Introduction

Erythrocytes perform  $\text{Na}^+/\text{Mg}^{2+}$  antiport, which is active in  $\text{Mg}^{2+}$ -loaded cells, and results in net  $\text{Mg}^{2+}$  efflux [1,2].  $\text{Na}^+/\text{Mg}^{2+}$  antiport in rat erythrocytes was previously thought to be irreversible, operating only as  $\text{Mg}^{2+}$  efflux coupled to  $\text{Na}^+$  influx [1]. In those earlier experiments, rat erythrocytes were loaded with  $\text{Na}^+$  and reincubated in  $\text{Na}^+$ -free,  $\text{Mg}^{2+}$ -containing medium. However,  $\text{Na}^+/\text{Mg}^{2+}$  antiport takes place only in  $\text{Mg}^{2+}$ -loaded cells [1–3], indicating that  $\text{Na}^+/\text{Mg}^{2+}$  antiport must be activated by increased intracellular  $\text{Mg}^{2+}$  concentration. Therefore, we investigated whether  $\text{Na}^+/\text{Mg}^{2+}$  antiport can be reversed in  $\text{Na}^+$ -loaded rat erythrocytes following additional  $\text{Mg}^{2+}$  loading.

## 2. Materials and methods

### 2.1. Cell loading

Blood was taken from anaesthetized rats (50 mg/kg Nembutal i.p.) by heart puncture with a heparinized sy-

ringe and centrifuged at  $1000 \times g$  for 10 min. The plasma and buffy coat were aspirated and the red cells were washed twice in 150 mM NaCl. Each experiment was done with erythrocytes from a single rat.

The cells were loaded with  $\text{Na}^+$  and  $\text{Mg}^{2+}$  by incubating a 10% cell suspension for 20 min at  $37^\circ\text{C}$  and for additional 20 min at  $0^\circ\text{C}$  in a high [NaCl] medium (150 mM NaCl, 5 mM glucose, 30 mM Hepes/Tris, pH 7.4) with the addition of 0.5–3.0 mM  $\text{MgCl}_2$ , 6  $\mu\text{M}$  A23187 (Boehringer-Mannheim) and 30  $\mu\text{g/ml}$  nystatin (Sigma), both dissolved in dimethyl sulfoxide. For removal of A23187 and nystatin, the cells were incubated four times in NaCl medium with the same  $\text{Mg}^{2+}$  concentration as in the loading medium plus 1% bovine serum albumin (Serva) for 10 min at  $37^\circ\text{C}$ . The NaCl medium was removed by washing the cells twice with cold choline Cl medium (150 mM choline Cl, 5 mM glucose, 30 mM Hepes/Tris, pH 7.4))

### 2.2. $\text{Mg}^{2+}$ transport

$\text{Mg}^{2+}$  transport was measured by reincubating a 10% suspension of  $\text{Na}^+ + \text{Mg}^{2+}$ -loaded cells at  $37^\circ\text{C}$  in media containing 5 mM glucose, 30 mM Hepes/Tris, pH 7.4, with various  $\text{Na}^+$  and  $\text{Mg}^{2+}$  content, as indicated.  $\text{Na}^+$  was isoosmotically substituted with choline Cl. At the beginning of reincubation and after different time points, as indicated, 0.5 ml aliquots of the cell suspensions were

Abbreviations:  $[\text{Mg}^{2+}]_o$ ,  $[\text{Mg}^{2+}]_i$ , extracellular, intracellular  $\text{Mg}^{2+}$  concentration;  $[\text{Na}^+]_o$ ,  $[\text{Na}^+]_i$ , extracellular, intracellular  $\text{Na}^+$  concentration;  $\text{pH}_i$ , intracellular pH; [ATP], cellular ATP concentration; PMA, phorbol myristate acetate; db-cAMP, dibutyryl cAMP; TCA, trichloroacetic acid.

<sup>\*</sup> Corresponding author. Fax: +49 30 8384802.

centrifuged for 0.5 min at  $10\,000 \times g$ . For  $\text{Mg}^{2+}$  determination, 100  $\mu\text{l}$  supernatant was diluted with 1 ml 5% TCA/0.175%  $\text{LaCl}_3$  and  $\text{Mg}^{2+}$  was measured by atomic absorption spectrophotometry (Philips, SP9).  $\text{Mg}^{2+}$  influx or  $\text{Mg}^{2+}$  efflux were calculated from the alterations in extracellular  $\text{Mg}^{2+}$  concentration and were related to the cell volume measured by haematocrit.

### 2.3. $\text{Na}^+$ efflux

$\text{Na}^+$  efflux was determined from the same supernatants by flame photometry (KLiNa, Beckman). For correction of  $\text{Mg}^{2+}$ -independent  $\text{Na}^+$  efflux, controls were run with  $\text{Mg}^{2+}$ -free incubation medium.

### 2.4. Cellular $\text{Mg}^{2+}$ , $\text{Ca}^{2+}$ , $\text{Mn}^{2+}$ and $\text{Na}^+$ content

For measuring cellular  $\text{Mg}^{2+}$ ,  $\text{Ca}^{2+}$ ,  $\text{Mn}^{2+}$  and  $\text{Na}^+$  contents, the cells were washed twice with 150 mM choline Cl and deproteinized with 5% TCA/0.175%  $\text{LaCl}_3$ .  $\text{Mg}^{2+}$ ,  $\text{Ca}^{2+}$  and  $\text{Mn}^{2+}$  contents of the supernatants were measured by atomic absorption spectrophotometry,  $\text{Na}^+$  content by flame photometry.

### 2.5. Cellular ATP content

ATP content of normal and ATP-depleted erythrocytes was determined enzymatically in TCA extracts by the luciferase method, according to the instructions of the manufacturer (Boehringer-Mannheim, No. 567 736).

Cells were ATP-depleted by addition of 5 mM 2-deoxyglucose instead of glucose and 1 mM iodoacetate during washing and incubation of the cells. Control experiments without iodoacetate revealed a smaller decrease of ATP but no effect of iodoacetate on  $\text{Mg}^{2+}$  transport.

## 3. Results

### 3.1. Induction of $\text{Mg}^{2+}$ uptake

When  $\text{Na}^+$  +  $\text{Mg}^{2+}$ -loaded rat erythrocytes were incubated in a high  $[\text{NaCl}]$  medium, net  $\text{Mg}^{2+}$  efflux occurred, which decreased with increasing  $[\text{Mg}^{2+}]_o$  (Fig. 1), as found in previous experiments [1]. However, when the  $\text{Na}^+$  +  $\text{Mg}^{2+}$ -loaded cells were incubated in choline Cl medium, containing 0.5 mM  $\text{Na}^+$ , the cells took up  $\text{Mg}^{2+}$  (Fig. 1). In cells, that were not loaded with  $\text{Mg}^{2+}$ , there was no  $\text{Mg}^{2+}$  uptake (data not shown). These results show that  $\text{Mg}^{2+}$  uptake can be induced in  $\text{Mg}^{2+}$ -loaded rat erythrocytes when the  $\text{Na}^+$  gradient was in the direction  $\text{high}_i/\text{low}_o$ .

### 3.2. Effect of $[\text{Mg}^{2+}]_o$ and $[\text{Mg}^{2+}]_i$ on $\text{Mg}^{2+}$ uptake

The rate of  $\text{Mg}^{2+}$  uptake was dependent on  $[\text{Mg}^{2+}]_o$ , obeying Michaelis-Menten kinetics with a  $K_m$  of 0.3 mM

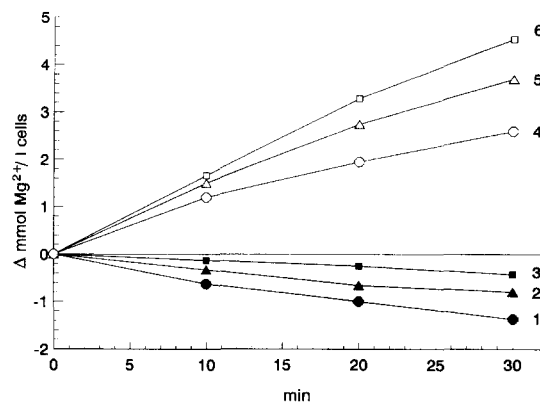


Fig. 1. Net  $\text{Mg}^{2+}$  efflux (below zero line) and net  $\text{Mg}^{2+}$  influx (above zero line) in  $\text{Na}^+$  +  $\text{Mg}^{2+}$ -loaded rat erythrocytes. The cells were loaded with 6  $\mu\text{M}$  A23187 and 30  $\mu\text{g}/\text{ml}$  nystatin in the presence of 3 mM  $\text{MgCl}_2$  and 150 mM  $\text{NaCl}$  ( $[\text{Na}^+]_i = 73 \pm 2$  mM).  $\text{Mg}^{2+}$  transport was measured in  $\text{NaCl}$  medium with 150 mM  $\text{NaCl}$  and 0.5 mM  $\text{MgCl}_2$  (1), 1.5 mM  $\text{MgCl}_2$  (2), and 3.0 mM  $\text{MgCl}_2$  (3), resulting in  $\text{Mg}^{2+}$  efflux, or in choline Cl medium with 0.5 mM  $\text{NaCl}$  and 0.5 mM  $\text{MgCl}_2$  (4), 1.5 mM  $\text{MgCl}_2$  (5), and 3.0 mM  $\text{MgCl}_2$  (6), resulting in  $\text{Mg}^{2+}$  influx. Mean of two experiments was plotted.

(not shown).  $\text{Mg}^{2+}$  uptake was also increased with  $\text{Mg}^{2+}$  loading (Fig. 2). When the values of Fig. 2, measured at  $[\text{Na}^+]_o = 0.5$  mM, were analyzed according to Hill as a function of  $[\text{Mg}^{2+}]_o$  during  $\text{Mg}^{2+}$  loading, a Hill coefficient of  $2.2 \pm 0.2$  was obtained (Fig. 3, curve A).

### 3.3. Effect of the $\text{Na}^+$ gradient on $\text{Mg}^{2+}$ transport

To analyze further the kinetics of net  $\text{Mg}^{2+}$  influx, we investigated net  $\text{Mg}^{2+}$  transport of  $\text{Na}^+$ -loaded cells ( $[\text{Na}^+]_i = 73 \pm 2$  mM, mean  $\pm$  S.E.,  $n = 6$ ) which were simultaneously  $\text{Mg}^{2+}$ -loaded at  $[\text{Mg}^{2+}]_o = 0.5$ –3.0 mM by replotting the values of Fig. 2 as a function of  $[\text{Na}^+]_i/[\text{Na}^+]_o$  (Fig. 4). Cellular  $\text{Mg}^{2+}$  content amounted to 2.0 mmol/l cells at  $[\text{Mg}^{2+}]_o = 0.5$  mM up to 4.9

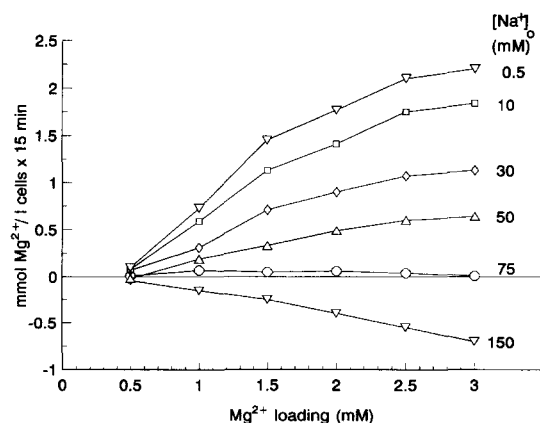


Fig. 2. Net  $\text{Mg}^{2+}$  efflux (below zero line) and net  $\text{Mg}^{2+}$  influx (above zero line) in  $\text{Na}^+$  +  $\text{Mg}^{2+}$ -loaded rat erythrocytes as a function of  $\text{Mg}^{2+}$  loading. The cells were loaded in the presence of 0.5–3.0 mM  $\text{MgCl}_2$  and 150 mM  $\text{NaCl}$ . Reincubation was performed in media with 1 mM  $\text{MgCl}_2$  and 0.5, 10, 30, 50, 75, and 150 mM  $\text{NaCl}$  as indicated.  $\text{NaCl}$  was isoosmotically substituted by choline Cl. Mean of two experiments.

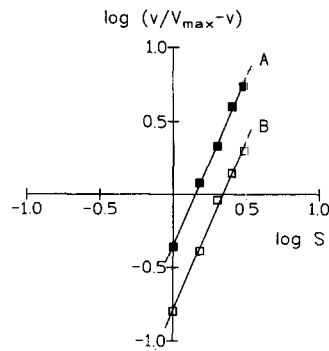


Fig. 3. Hill plot ( $\log(v/V_{\max} - v) = n \log S - \log K'$ ) of  $\text{Mg}^{2+}$  uptake by  $\text{Na}^+$  +  $\text{Mg}^{2+}$ -loaded rat erythrocytes.  $\log(v/V_{\max} - v)$  was plotted as a function of  $[\text{Mg}^{2+}]_o$  in the loading medium. (A) Rat erythrocytes with normal ATP content. Values measured at 0.5 mM NaCl and 1 mM  $\text{MgCl}_2$  were taken from Fig. 2. (B) ATP-depleted rat erythrocytes. Analogous values were taken from Fig. 6.

mmol/l cells at  $[\text{Mg}^{2+}]_o = 3.0$  mM, as found in previous experiments [1]. After reincubation in medium with  $[\text{Na}^+]_o = 150$  mM, giving  $[\text{Na}^+]_i/[\text{Na}^+]_o = 0.49$ , net  $\text{Mg}^{2+}$  efflux occurred. Its rate rose with increasing  $\text{Mg}^{2+}$ -loading as characterized in previous experiments [1]. In media with  $[\text{Na}^+]_o < 75$  mM, giving  $[\text{Na}^+]_i/[\text{Na}^+]_o > 1$ , net  $\text{Mg}^{2+}$  efflux switched to net  $\text{Mg}^{2+}$  influx. Its rate increased with  $\text{Mg}^{2+}$  loading and with increasing  $[\text{Na}^+]_i/[\text{Na}^+]_o$  (Fig. 4).

These results show: (1) The increased rate of  $\text{Mg}^{2+}$  uptake with  $\text{Mg}^{2+}$  loading (Figs. 2, 4), indicates that the increase in  $[\text{Mg}^{2+}]_i$  activated the  $\text{Mg}^{2+}$  influx system. According to Fig. 3 this activation was brought about by a co-operative effect.

(2) The intracellular/extracellular  $\text{Na}^+$  gradient contributes to the driving force of  $\text{Mg}^{2+}$  uptake. As shown in Fig. 4, at  $[\text{Na}^+]_i/[\text{Na}^+]_o = 1$ , there was no net  $\text{Mg}^{2+}$

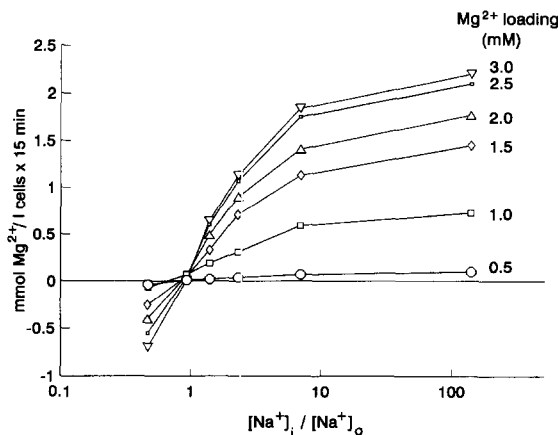


Fig. 4. Net  $\text{Mg}^{2+}$  efflux (below zero line) and net  $\text{Mg}^{2+}$  influx (above zero line) in  $\text{Na}^+$  +  $\text{Mg}^{2+}$ -loaded rat erythrocytes as a function of the  $\text{Na}^+$  gradient. Same experiments as in Fig. 2. The cells were differently loaded with  $\text{Mg}^{2+}$  as indicated.  $\text{Mg}^{2+}$  transport was plotted as a function of  $[\text{Na}^+]_i/[\text{Na}^+]_o$  (log scale),  $[\text{Na}^+]_i = 73 \pm 2$  mM.

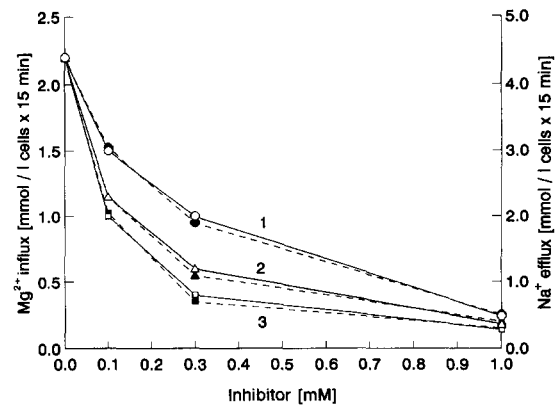


Fig. 5. Inhibition of net  $\text{Mg}^{2+}$  influx and net  $\text{Na}^+$  efflux of  $\text{Na}^+$  +  $\text{Mg}^{2+}$ -loaded rat erythrocytes by amiloride (1), imipramine (2) and quinidine (3). The cells were loaded in the presence of 3 mM  $\text{MgCl}_2$  and 150 mM NaCl. Reincubation in choline Cl medium with 0.5 mM NaCl and 1 mM  $\text{MgCl}_2$ .  $\text{Na}^+$  efflux was corrected for passive ( $\text{Mg}^{2+}$ -independent)  $\text{Na}^+$  leak by subtraction of  $\text{Na}^+$  leak in  $\text{Mg}^{2+}$ -free reincubation medium. Open symbols (solid line), net  $\text{Mg}^{2+}$  influx; filled symbols (dashed line), net  $\text{Na}^+$  efflux. Mean of two experiments.

transport. At  $[\text{Na}^+]_i/[\text{Na}^+]_o > 1$ , net  $\text{Mg}^{2+}$  influx occurred, whereas at  $[\text{Na}^+]_i/[\text{Na}^+]_o < 1$  net  $\text{Mg}^{2+}$  efflux was observed. The curves of  $\text{Mg}^{2+}$  transport cross the zero line of net  $\text{Mg}^{2+}$  flux at  $[\text{Na}^+]_i/[\text{Na}^+]_o = 1$ . Within experimental error, the curves (Fig. 4) have the same slope below and above the crossing point. This result is evidence that the action of the  $\text{Na}^+$  gradient is the same on each side of the membrane. Moreover, since the crossing point is at  $[\text{Na}^+]_i/[\text{Na}^+]_o = 1$ , net  $\text{Mg}^{2+}$  flux under the used conditions may only depend on the  $\text{Na}^+$  gradient.

When  $\text{Mg}^{2+}$ -loaded rat erythrocytes were loaded in the presence of 75 mM  $\text{Na}^+$  instead of 150 mM resulting in  $[\text{Na}^+]_i = 25$  mM and incubated at various  $[\text{Na}^+]_o$  the rate of  $\text{Mg}^{2+}$  transport as a function of the  $\text{Na}^+$  gradient was identical (data not shown). Again, this result shows that the  $\text{Na}^+$  gradient contributes to the driving force for  $\text{Mg}^{2+}$  transport in  $\text{Mg}^{2+}$ -loaded rat erythrocytes.

### 3.4. $\text{Na}^+$ coupling of $\text{Mg}^{2+}$ uptake

During  $\text{Mg}^{2+}$  uptake,  $\text{Na}^+$  is released from  $\text{Na}^+$  +  $\text{Mg}^{2+}$ -loaded rat erythrocytes.  $\text{Mg}^{2+}$  uptake and  $\text{Na}^+$  release were inhibited by amiloride, imipramine and quinidine (Fig. 5). Each of these substances inhibited  $\text{Mg}^{2+}$  uptake and  $\text{Na}^+$  release to the same extent, indicating that net  $\text{Mg}^{2+}$  influx is coupled to net  $\text{Na}^+$  efflux. The stoichiometric ratio can be obtained by comparing the rate of  $\text{Mg}^{2+}$  uptake and  $\text{Na}^+$  release. From the scales in Fig. 5 it can be seen that the stoichiometric ratio is 2  $\text{Na}^+$  for 1  $\text{Mg}^{2+}$ . Hence, the stoichiometry is the same as was found for  $\text{Na}^+/\text{Mg}^{2+}$  antiport from  $\text{Mg}^{2+}$ -loaded rat erythrocytes [1].

From Fig. 5 the  $K_i$  values can be obtained.  $K_i$  for amiloride amounts to 0.3 mM, for imipramine to 0.15 mM and for quinidine to 0.1 mM. These values correspond to

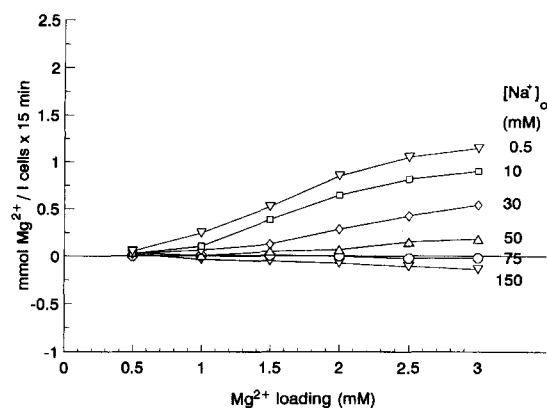


Fig. 6.  $\text{Mg}^{2+}$  transport in  $\text{Na}^+$  +  $\text{Mg}^{2+}$ -loaded, ATP-depleted rat erythrocytes as a function of  $\text{Mg}^{2+}$  loading. The cells were loaded in the presence of 0.5–3.0 mM  $\text{MgCl}_2$  and 150 mM NaCl, resulting in  $[\text{Na}^+]_i = 72 \pm 2$  mM. Reincubation was performed in media with 0.5, 30, 50, 75 and 150 mM NaCl and 1 mM  $\text{MgCl}_2$  with the addition of 5 mM 2-deoxyglucose instead of glucose and 1 mM iodoacetate for ATP depletion. Analogous experiments as in Fig. 4. Mean of two experiments.

the  $K_i$  values which were obtained for inhibition of net  $\text{Mg}^{2+}$  efflux via  $\text{Na}^+$  /  $\text{Mg}^{2+}$  antiport [4].

### 3.5. Role of ATP in $\text{Mg}^{2+}$ uptake

Net  $\text{Mg}^{2+}$  efflux via  $\text{Na}^+$  /  $\text{Mg}^{2+}$  antiport in rat erythrocytes was dependent on ATP [1]. Its function has not been defined so far. The function of ATP in net  $\text{Mg}^{2+}$  influx was analyzed by repeating the experiment shown in Figs. 2 and 4 with ATP-depleted cells. Incubating  $\text{Na}^+$  +  $\text{Mg}^{2+}$ -loaded cells with 5 mM 2-deoxyglucose plus 1 mM iodoacetate instead of glucose reduced ATP content by 85% (from 0.6 to 0.09 mmol/l cells). The results with ATP-depleted cells were similar to those obtained from control cells. Again,  $\text{Mg}^{2+}$  uptake was increased with  $\text{Mg}^{2+}$  loading of the cells and with the  $\text{Na}^+$  gradient (Figs. 6 and 7). However, the rates of  $\text{Mg}^{2+}$  flux were

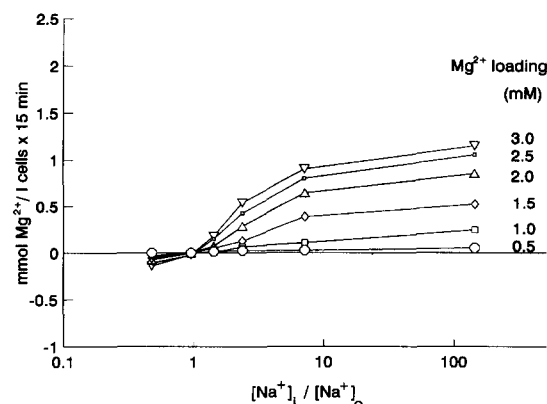


Fig. 7.  $\text{Mg}^{2+}$  transport in  $\text{Na}^+$  +  $\text{Mg}^{2+}$ -loaded, ATP-depleted rat erythrocytes as a function of the  $\text{Na}^+$  gradient (log scale). Same experiments as in Fig. 6.  $[\text{Na}^+]_i = 72 \pm 2$  mM.

Table 1  
Regulation of  $\text{Mg}^{2+}$  uptake by rat erythrocytes

Addition	M	$\text{Mg}^{2+}$ uptake (mmol $\text{Mg}^{2+}$ / 1 cells per 30 min)
Control	—	$1.50 \pm 0.09$
PMA	$10^{-6}$	$1.91 \pm 0.11^a$
Staurosporine	$10^{-7}$	$0.94 \pm 0.10^b$
Okadaic acid	$10^{-6}$	$1.72 \pm 0.04^a$
db-cAMP	$10^{-4}$	$1.51 \pm 0.08$
PMA	$10^{-6}$	
+ staurosporine	$10^{-7}$	$0.99 \pm 0.04^b$
PMA	$10^{-6}$	
+ okadaic acid	$10^{-6}$	$1.99 \pm 0.02^b$

The cells were loaded in the presence of 150 mM NaCl and 1 mM  $\text{MgCl}_2$ .  $\text{Mg}^{2+}$  uptake was measured in choline Cl medium with 0.5 mM NaCl and 1 mM  $\text{MgCl}_2$ . Mean  $\pm$  S.E. of four experiments. Significant differences to controls by unpaired Student's *t*-test. <sup>a</sup>  $P < 0.05$ , <sup>b</sup>  $P < 0.01$ .

lower than those in control cells (Figs. 2 and 4). In accordance with this result, in ATP-depleted cells,  $V_{\max}$  of  $\text{Mg}^{2+}$  uptake was reduced by 33% (data not shown). When the rate of  $\text{Mg}^{2+}$  uptake in ATP-depleted cells, measured at  $[\text{Na}^+]_o = 0.5$  mM (Fig. 6), was analyzed according to Hill as a function of  $[\text{Mg}^{2+}]_o$  during  $\text{Mg}^{2+}$  loading, a Hill coefficient of 2 was obtained (Fig. 3, curve B). The same Hill coefficient was found in control cells (Fig. 3, curve A). However,  $\log K'$  was increased in ATP-depleted cells by  $\Delta \log K' = 0.48$  (factor of 3) (Fig. 3), indicating a lower affinity of  $[\text{Mg}^{2+}]_i$ . For further characterisation of the function of ATP, we tested the effect of protein phosphorylation by protein kinase A (activated by db-cAMP) and protein kinase C (activated by PMA) which are both inhibited by staurosporine [5]. Moreover, the involvement of phosphorylated protein was tested by addition of okadaic acid, which inhibits Ser/Thr-protein phosphatases 1 and 2A [6,7]. As shown in Table 1,  $\text{Mg}^{2+}$  uptake was stimulated by PMA and inhibited by staurosporine. Okadaic acid had a small stimulatory effect, and db-cAMP was ineffective, indicating stimulation by protein kinase C. Stimulation of  $\text{Mg}^{2+}$  uptake by PMA was less expressed in cells loaded in the presence of 3.0 mM  $\text{MgCl}_2$  compared to 1.0 mM  $\text{MgCl}_2$  (data not shown).

### 3.6. Cation specificity of $\text{Mg}^{2+}$ uptake

In previous experiments with  $\text{Mg}^{2+}$ -loaded rat erythrocytes additional  $\text{Ca}^{2+}$  loading had no significant effect on  $\text{Mg}^{2+}$  efflux via  $\text{Na}^+$  /  $\text{Mg}^{2+}$  antiport [8]. However, in these experiments  $\text{Ca}^{2+}$  loading was limited due to an effective  $\text{Ca}^{2+}$  pump which prevented sufficient  $\text{Ca}^{2+}$  loading.

Reversibility of  $\text{Na}^+$  /  $\text{Mg}^{2+}$  antiport offers the possibility to test cation specificity by extracellular addition of divalent cations, which would be toxic when applied intracellularly. As shown in Fig. 8,  $\text{Mg}^{2+}$  uptake was inhibited by  $\text{Ca}^{2+}$ ,  $\text{Mn}^{2+}$ ,  $\text{Ni}^{2+}$ , and  $\text{La}^{3+}$ . At the used concentrations,  $\text{Sr}^{2+}$  did not affect  $\text{Mg}^{2+}$  uptake.

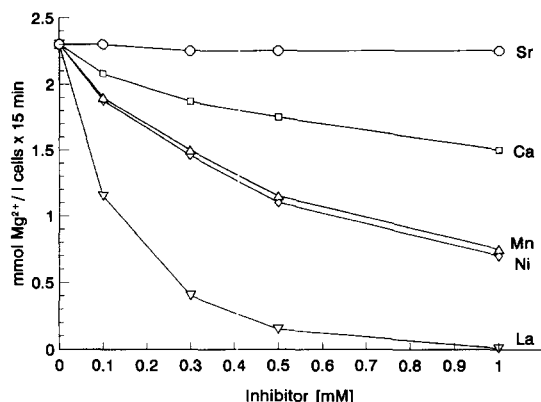


Fig. 8. Inhibition of  $\text{Mg}^{2+}$  uptake in  $\text{Na}^+ + \text{Mg}^{2+}$ -loaded rat erythrocytes by extracellular  $\text{SrCl}_2$ ,  $\text{CaCl}_2$ ,  $\text{MnCl}_2$ ,  $\text{NiSO}_4$  and  $\text{LaCl}_3$ . The cells were loaded in the presence of 3 mM  $\text{MgCl}_2$  and 150 mM  $\text{NaCl}$  and reincubated in choline Cl medium with 0.5 mM  $\text{NaCl}$  and 1.3 mM  $\text{MgCl}_2$ . Mean of two experiments.

Using Dixon plots the inhibition was defined as being competitive (not shown). The  $K_i$  values amounted to 0.4 mM for  $\text{Ca}^{2+}$ , 0.02 mM for  $\text{Mn}^{2+}$  and  $\text{Ni}^{2+}$ , and to 0.005 mM for  $\text{La}^{3+}$ .  $\text{Mn}^{2+}$  was taken up by the cells (data not shown). Also, in preceding experiments  $\text{Mn}^{2+}$  was taken up by rat erythrocytes in exchange for  $\text{Mg}^{2+}$  via  $\text{Na}^+/\text{Mg}^{2+}$  antiport [9,10], indicating that  $\text{Mn}^{2+}$  can substitute for  $\text{Mg}^{2+}$  in  $\text{Na}^+/\text{Mg}^{2+}$  antiport.  $\text{Ca}^{2+}$  was not taken up by the cells (data not shown). Uptake of  $\text{Sr}^{2+}$ ,  $\text{Ni}^{2+}$  and  $\text{La}^{3+}$  via  $\text{Na}^+/\text{Mg}^{2+}$  antiport was not investigated.

### 3.7. Cell type specificity of $\text{Mg}^{2+}$ uptake

In analogous experiments human erythrocytes were loaded with  $\text{Na}^+$  and  $\text{Mg}^{2+}$ . However, under identical conditions human erythrocytes did not perform  $\text{Mg}^{2+}$  uptake (data not shown). In similar experiments, also Schatzmann [11] could not obtain  $\text{Mg}^{2+}$  uptake in human erythrocytes, whereas in ferret erythrocytes  $\text{Na}^+/\text{Mg}^{2+}$  antiport could be reversed by reversing the  $\text{Na}^+$  gradient [12,13]. These results show that in erythrocytes  $\text{Na}^+/\text{Mg}^{2+}$  antiporters are existing with different species-dependent properties.

## 4. Discussion

The results have shown that rat erythrocytes can be induced to take up extracellular  $\text{Mg}^{2+}$  in exchange for intracellular  $\text{Na}^+$ . Prerequisite is:

- (1) The cells must be loaded with  $\text{Mg}^{2+}$ ,
- (2)  $[\text{Na}^+]_i/[\text{Na}^+]_o$  must be  $> 1$ .

In rat erythrocytes the  $\text{Na}^+$  gradient contributes to the driving force for net  $\text{Mg}^{2+}$  transport. Additionally, 2 intracellular  $\text{Na}^+$  are exchanged for 1 extracellular  $\text{Mg}^{2+}$  in  $\text{Mg}^{2+}$  uptake. The same stoichiometric ratio holds for net  $\text{Mg}^{2+}$  efflux via  $\text{Na}^+/\text{Mg}^{2+}$  antiport [1].

Net  $\text{Mg}^{2+}$  influx coupled to net  $\text{Na}^+$  efflux was inhibited by about the same degree as net  $\text{Mg}^{2+}$  efflux via  $\text{Na}^+/\text{Mg}^{2+}$  antiport by amiloride, imipramine and quinidine. Moreover,  $\text{Mn}^{2+}$  inhibited  $\text{Mg}^{2+}$  uptake competitively and was taken up itself by  $\text{Na}^+/\text{Mg}^{2+}$  antiport [9,10]. These results suggest that  $\text{Na}^+/\text{Mg}^{2+}$  antiport in rat erythrocytes can operate reversibly.

A prerequisite for demonstrating reversible  $\text{Na}^+/\text{Mg}^{2+}$  antiport in rat erythrocytes was  $\text{Mg}^{2+}$  loading. Net  $\text{Mg}^{2+}$  efflux via  $\text{Na}^+/\text{Mg}^{2+}$  antiport was also only seen in  $\text{Mg}^{2+}$ -loaded cells [1]. In rat erythrocytes, net  $\text{Mg}^{2+}$  efflux as a function of  $[\text{Mg}^{2+}]_i$  revealed a Hill coefficient of 2.44 [1]. This result was explained by the assumption that 1 intracellular  $\text{Mg}^{2+}$  is released in exchange for 2 extracellular  $\text{Na}^+$  in  $\text{Na}^+/\text{Mg}^{2+}$  antiport and that 2 additional intracellular  $\text{Mg}^{2+}$  are operating co-operatively to activate the  $\text{Na}^+/\text{Mg}^{2+}$  antiporter. In the present experiments, the Hill coefficient for net  $\text{Mg}^{2+}$  influx amounted to 2.2, again indicating that 2 intracellular  $\text{Mg}^{2+}$  are needed in  $\text{Mg}^{2+}$  uptake via reversible  $\text{Na}^+/\text{Mg}^{2+}$  antiport. The increased  $\text{Mg}^{2+}$  uptake at increased  $\text{Mg}^{2+}$  loading (Fig. 2) fits into this scheme, indicating that more  $\text{Na}^+/\text{Mg}^{2+}$  antiporter molecules are activated by increasing  $[\text{Mg}^{2+}]_i$ . The  $\text{Na}^+/\text{Mg}^{2+}$  antiporter may have different  $\text{Mg}^{2+}$  sites: two intracellular  $\text{Mg}^{2+}$  binding sites for activating  $\text{Na}^+/\text{Mg}^{2+}$  antiport, an intracellular  $\text{Mg}^{2+}$  binding site for  $\text{Mg}^{2+}$  efflux and an extracellular  $\text{Mg}^{2+}$  binding site for  $\text{Mg}^{2+}$  influx. Whether the extracellular and intracellular  $\text{Mg}^{2+}$  transport site of the  $\text{Na}^+/\text{Mg}^{2+}$  antiporter in rat erythrocytes is operating with the same or with different affinity at both sides of the membrane cannot be decided because of the co-operative action of  $[\text{Mg}^{2+}]_i$  in  $\text{Mg}^{2+}$  transport.

The role of ATP in net  $\text{Mg}^{2+}$  influx is to increase the affinity of the  $\text{Na}^+/\text{Mg}^{2+}$  antiporter for intracellular  $\text{Mg}^{2+}$ . Taking into account the co-operative function of  $[\text{Mg}^{2+}]_i$  (Fig. 3) the possible action of ATP may be phosphorylation of the  $\text{Na}^+/\text{Mg}^{2+}$  antiporter by  $\text{MgATP}$  and increased binding of  $\text{Mg}^{2+}$  to a modifier site of the phosphorylated  $\text{Na}^+/\text{Mg}^{2+}$  antiporter. At lower cellular ATP, less  $\text{Na}^+/\text{Mg}^{2+}$  antiporters may be activated, resulting in lower  $V_{\max}$  of  $\text{Mg}^{2+}$  uptake. This mechanism is in agreement with the stimulation of  $\text{Mg}^{2+}$  uptake by PMA and okadaic acid and its inhibition by staurosporine (Table 1), indicating that protein kinase C may phosphorylate the  $\text{Na}^+/\text{Mg}^{2+}$  antiporter or a protein, which is involved in  $\text{Mg}^{2+}$  uptake. This mechanism may represent regulation of  $\text{Na}^+/\text{Mg}^{2+}$  antiport. As shown by other experiments [7,14] PMA and okadaic acid enhance protein phosphorylation in erythrocytes. The results indicate that  $\text{Na}^+/\text{Mg}^{2+}$  antiport has very similar properties to  $\text{Na}^+/\text{H}^+$  and  $\text{Na}^+/\text{Ca}^{2+}$  antiport.  $\text{Na}^+/\text{H}^+$  is silent at physiological  $\text{pH}_i$  but is activated when the cytoplasm becomes acidic which is mediated by the allosteric effect of an intracellular modifier site. Besides acidification  $\text{Na}^+/\text{H}^+$  antiport was activated by okadaic acid [6] and phorbol ester

[15] via phosphorylation which increases the affinity of the  $\text{Na}^+/\text{H}^+$  antiporter for  $\text{H}^+$  at the internal regulatory site [6,15,16]. Similarly, also  $\text{Na}^+/\text{Ca}^{2+}$  antiport is activated by increased  $[\text{Ca}^{2+}]_i$  and by phosphorylation [17–19]. Thus,  $\text{Na}^+/\text{Mg}^{2+}$  antiport of rat erythrocytes may have a similar structure to  $\text{Na}^+/\text{H}^+$  and  $\text{Na}^+/\text{Ca}^{2+}$  antiporters including their isoforms [16,17,20,21]. The physiological function of  $\text{Na}^+/\text{Mg}^{2+}$  antiport in vivo may be the performance of net  $\text{Mg}^{2+}$  efflux.  $[\text{Mg}^{2+}]_i$  is buffered [4] by reversible reaction with  $\text{Mg}^{2+}$ -binding ligands, particularly ATP. When  $[\text{Mg}^{2+}]_i$  is increased by release from  $\text{Mg}^{2+}$ -binding ligands which can occur by ATP depletion or acidification [22],  $\text{Mg}^{2+}$  can be transported out of the cell to support constancy of  $[\text{Mg}^{2+}]_i$  [22].  $\text{Mg}^{2+}$  uptake via  $\text{Na}^+/\text{Mg}^{2+}$  antiport may play no role because in vivo the  $\text{Na}^+$  gradient (e.g., in rat erythrocytes) does not become  $> 1$ .

## References

- [1] Günther, T., Vormann, J. and Höllriegel, V. (1990) *Biochim. Biophys. Acta* 1023, 455–461.
- [2] Günther, T., Vormann, J. and Förster, R. (1984) *Biochem. Biophys. Res. Commun.* 119, 124–131.
- [3] Günther, T. and Vormann, J. (1990) *Magnesium Trace Elem.* 9, 279–282.
- [4] Günther, T. (1993) *Min. Electr. Metab.* 19, 259–265.
- [5] Tamaoki, T., Nomoto, H., Takahashi, I., Kato, Y., Morimoto, M. and Tomita, F. (1986) *Biochem. Biophys. Res. Commun.* 135, 397–402.
- [6] Bianchini, L., Woodside, M., Sardet, C., Pouyssegur, J., Takai, A. and Grinstein, S. (1991) *J. Biol. Chem.* 266, 15406–15413.
- [7] Bordin, L., Clari, G., Bellato, M., Tessarin, C. and Moret, V. (1993) *Biochem. Biophys. Res. Commun.* 195, 723–729.
- [8] Günther, T. and Vormann, J. (1989) *FEBS Lett.* 250, 633–637.
- [9] Féray, J.C. and Garay, R. (1987) *J. Biol. Chem.* 262, 5763–5768.
- [10] Günther, T., Vormann, J. and Cragoe, Jr. E.J. (1990) *FEBS Lett.* 261, 47–51.
- [11] Schatzmann, H.J. (1993) *Biochim. Biophys. Acta* 1148, 15–18.
- [12] Flatman, P.W. and Smith, L.M. (1990) *J. Physiol.* 431, 11–25.
- [13] Flatman, P.W. and Smith, L.M. (1991) *J. Physiol.* 443, 217–230.
- [14] Cohen, C.M. and Foley, S.F. (1986) *J. Biol. Chem.* 261, 7701–7709.
- [15] Sardet, C., Counillon, L., Franchi, A. and Pouyssegur, J. (1990) *Science* 247, 723–726.
- [16] Levine, S.A., Montrose, M.H., Tse, M. and Donowitz, M. (1993) *J. Biol. Chem.* 268, 25527–25535.
- [17] Reeves, J.P. (1992) *Arch. Biochem. Biophys.* 292, 329–334.
- [18] Caroni, P. and Carafoli, E. (1985) *Eur. J. Biochem.* 132, 451–460.
- [19] DiPolo, R. and Beaugé, L. (1987) *Biochim. Biophys. Acta* 897, 347–354.
- [20] Tse, C.M., Brant, S.R., Walker, M.S., Pouyssegur, J. and Donowitz, M. (1992) *J. Biol. Chem.* 267, 9340–9346.
- [21] Nakasaki, Y., Iwamoto, T., Hanada, H., Imagawa, T. and Shigekawa, M. (1993) *J. Biochem.* 114, 528–534.
- [22] Günther, T. and Vormann, J. (1994) *Renal Physiol. Biochem.* 17, 279–286.